Journal of Alloys and Compounds 502 (2010) L1–L5

Contents lists available at ScienceDirect

Journal of Alloys and Compounds

journal homepage: www.elsevier.com/locate/jallcom

Letter

Reverse-microemulsion preparation of visible-light-driven nano-sized $BiVO_4$

Chen-Yang Chung, Chung-Hsin Lu*

Department of Chemical Engineering, National Taiwan University, Taipei, Taiwan, ROC

ARTICLE INFO

Article history:
Received 30 October 2009
Received in revised form 24 February 2010
Accepted 1 March 2010
Available online 7 March 2010

Keywords:
Chemical synthesis
Light absorption and reflection
Bismuth vanadate
Bismuth oxide
Photocatalysis
Methylene blue

ABSTRACT

Nano-scaled monoclinic bismuth vanadate was prepared via a novel reverse-microemulsion process. This process significantly reduced the calcination duration and heating temperatures required for preparing the pure phase in the conventional methods. The prepared powders had more uniform morphology and smaller grain sizes as compared with the powders obtained via the other routes. The average particle size of $BiVO_4$ was decreased to35 nm, thereby leading to improve photocatalytic properties under visible-light illumination. The reduced particle sizes can be ascribed to the presence of nano-scaled micelles that restrict the growth of the particles. This reverse-microemulsion process was demonstrated to be a promising method for synthesizing visible-light-driven $BiVO_4$ with enhanced photocatalytic activities.

1. Introduction

Photocatalysts have been widely used for pollutant degradation during the last two decades. TiO_2 is one of the most extensively investigated photocatalysts for degrading various chemical compounds because of its strong photocatalytic activity [1–4]. However, the practical application of TiO_2 is limited since it requires UV light activation.

Many researchers have devoted their efforts to find a suitable alternative for TiO_2. $BiVO_4$ is intensively investigated due to its excellent photocatalytic activity [5,6]. $BiVO_4$ has three different types of structures: tetragonal zircon, monoclinic scheelite and tetragonal scheelite [7]. Among these three types of structures, monoclinic scheelite has the strongest photocatalytic activity owing to its narrow band gap (ca. 2.4 eV) [7–9]. Several different methods for preparing monoclinic scheelite $BiVO_4$ have been developed, such as aqueous process [10,11], hydrothermal process [12], solution combustion synthesis method [13], and flame spray pyrolysis [14]. The ordered mesoporous $BiVO_4$ was synthesized via the nanocasting process, using mesoporous silica KIT-6 as the replica parent templates [5]. Furthermore, in order to enhance the activity of $BiVO_4$, the modification methods for doping metal [15–18] and metal oxide [19,20] have been used. However, these modification technologies have the drawbacks of complex processes. In addition, the particle sizes are still larger than 100 nm. It is known that the photocatalytic activity strongly relates to the particle size and surface area of the powders. Therefore, the synthesis of nano-sized $BiVO_4$ photocatalysts with high surface area is an important research subject to improve photocatalytic efficiency.

In order to reduce the particle size of $BiVO_4$, the reverse-microemulsion process was developed in this study. The reverse-microemulsion method is considered a feasible technique for synthesizing complex inorganic compounds having ultrafine particle sizes with controlled morphology. The micelles which confine the reactive species can restrict the particle growth. This method has been demonstrated to improve the characteristics of various kinds of ceramic materials [21]. In this study, the preparation and microstructure of microemulsion-derived $BiVO_4$ were investigated. The effects of processing temperatures on the photocatalytic properties of the obtained powders were also explored in detail.

2. Experimental

$BiVO_4$ powders were prepared via the reverse-microemulsion process. $Bi(NO_3)_3{\cdot}5H_2O$ and NH_4VO_3, with a molar ratio of 1:1, were dissolved in HNO_3 (1.2 M) to form a water phase. Cyclohexane, 1-hexanol (surfactant) and polyoxyethylene tert-octylphenyl ether (triton X-100, co-surfactant) were used to form an oil phase. The aqueous and oil phase solutions were mixed to form a transparent microemulsion solution, followed by dripping this formed solution into hot kerosene at 185 °C for evaporating water. The dried precursors were further heated at 400 °C in air for 2 h to remove any residual organics. The obtained powders were grounded and calcined at various temperatures in air for 20 min. For comparison, $BiVO_4$ was also prepared via the conventional solid-state (s.s.) reaction method. Bi_2O_3 and V_2O_5, with a molar ratio of 1:1, were mixed via ball-milling and the mixtures were calcined at 700 °C in air for 5 h to obtain the target powder.

The purity and crystallinity of the prepared powders were determined using powder X-ray diffraction method. Thermogravimetry analysis (TGA) was applied

---

* Corresponding author. Tel.: +886 2 23651428; fax: +886 2 23623040.
E-mail address: chlu@ntu.edu.tw (C.-H. Lu).

0925-8388/$ – see front matter © 2010 Elsevier B.V. All rights reserved.
doi:10.1016/j.jallcom.2010.03.013

for analyzing the reaction processes. The heating rate was set at 10 °C/min and alumina powder was used as a reference. The surface morphology and particle size of the prepared samples were examined using a scanning electron microscope and a transmission electron microscope. The diffuse reflectance spectra were measured via a UV–vis spectrophotometer. Methylene blue solutions were used to determine the photocatalytic activities of the prepared powders.

The photocatalyst of BiVO$_4$ was illuminated under visible light, using a 400 nm glass filter to cut off light with a wavelength shorter than 400 nm. The quantitative measurement of the methylene blue concentration was performed by recording the absorbance peak of methylene blue at 664 nm using an UV–vis spectrophotometer.

3. Results and discussion

3.1. Characterization of BiVO$_4$

Fig. 1 illustrates the XRD patterns of microemulsion-derived BiVO$_4$ powders calcined at different temperatures and the solid-state derived BiVO$_4$ powders heated at 700 °C for 5 h. After heating at 400 °C for 10 min, a large amount of BiVO$_4$ was formed with an impurity phase of $Bi_6V_3O_{16}$ (Fig. 1(a)). With further heating at 400 °C for 20 min, $Bi_6V_3O_{16}$ completely disappeared and a pure phase of BiVO$_4$ was formed (Fig. 1(b)) as confirmed by the fact that all of the diffraction peaks were consistent with the data listed for monoclinic BiVO$_4$ in ICDD file No.: 83-1698 [22]. When the heating temperature was raised, the crystallinity of the powders enhanced gradually as shown in Fig. 1(c)–(e). As a comparison, the conventional solid-state process was also adopted to synthesize BiVO$_4$. The XRD pattern of the solid-state derived BiVO$_4$ powders heated at 700 °C for 5 h is illustrated in Fig. 1(f). The crystallinity of the obtained powders was slightly higher than that of the microemulsion-derived BiVO$_4$ heated at 700 °C. It was found that heating at 700 °C for 5 h is required to obtain pure BiVO$_4$. Therefore, the reverse-microemulsion method, as compared with the solid-state process, significantly reduced the heating temperature from 700 to 400 °C and the calcination duration from 5 h to 20 min. The above mentioned advantages can be ascribed to the unique characteristics of the microemulsion process. In the microemulsion system, water-in-oil micelles are formed. Constituent ions are restricted in tiny micelles which are stabilized by the surfactants and co-surfactants. The presence of numerous nano-scaled micelles significantly shortens the intermolecular diffusion distance between reactants, leading to an enhancement in the precursor activity. Accordingly, the chemical reaction can be markedly facilitated via the microemulsion process [23–27].

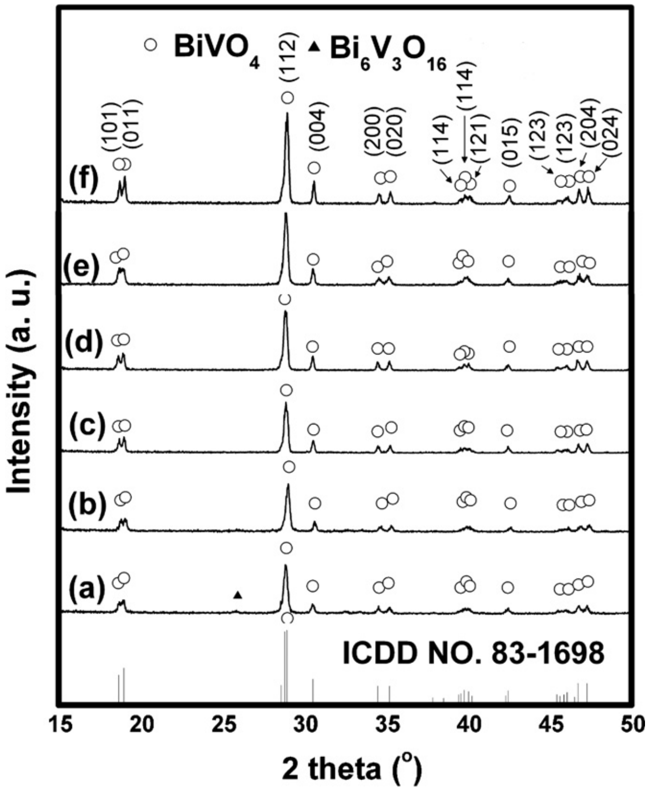

Fig. 1. X-ray diffraction patterns of microemulsion-derived BiVO$_4$ powders heated at (a) 400 °C for 10 min, (b) 400, (c) 500, (d) 600 and (e) 700 °C for 20 min and the solid-state derived BiVO$_4$ powders heated at (f) 700 °C for 5 h.

The microemulsion-derived precursors were examined via TGA. Two stages of weight loss were found: the first stage occurred at 100 °C which was due to dehydration; while the second stage occurred at temperature ranging from 350 to 550 °C owing to the removal of residual organic and BiVO$_4$ formation. No further weight loss was observed at temperatures higher than 550 °C, implying the complete formation of BiVO$_4$.

3.2. Microstructures of BiVO$_4$

Fig. 2 shows the microstructures of BiVO$_4$ powders synthesized via different methods. After heating at 400 °C for 20 min, the particle size of the microemulsion-derived samples was around 35 nm (Fig. 2(a)). The corresponding TEM photograph is shown in Fig. 2(e). These images confirm that nano-sized BiVO$_4$ powders were successfully synthesized in this study. In the inset of Fig. 2(e), the presence of several obvious diffraction spots reveals the formation of well-crystallized grains. When the heating temperature was raised to 500, 600 and 700 °C, the sizes of the particles grew respectively to 220, 250 and 750 nm (Fig. 2(b)–(d)). The microstructure of the solid-state derived BiVO$_4$ (Fig. 2(f)) powders exhibit an irregular shape. The particle size was around 700 nm, and the powders were greatly aggregated with each other. As compared with the solid-state process that produces micrometer-sized BiVO$_4$ powders, the reverse-microemulsion method is successful in synthesizing substantially smaller BiVO$_4$ particles in nanometer order. This result is attributed to the restriction effects of nano-scaled micelles on particle growth that in term lead to the formation of the nano-sized powders [28]. The crystal sizes of the prepared powders were calculated according to Debye–Scherrer's formula [29]:

$$D = \frac{K\lambda}{(B^2 - b^2)^{0.5} \cos\theta} \tag{1}$$

where D is the crystal size; λ represents the wavelength of X-ray radiation ($\lambda = 0.15418$ nm); K is usually taken as 0.89; B and b are the peak widths of the half-maximum height of the sample and of the equipment broadening, respectively. The crystal sizes of BiVO$_4$ powders calcined at 400, 500, 600 and 700 °C were determined to be 29.7, 37.7, 40.1 and 41.1 nm, respectively. This result indicates that crystal sizes increased with heating temperatures. As compared with the data shown in Fig. 2, it is quite obvious that the average particle and crystal sizes were nearly equal when the heating temperature was 400 °C. However, as the heating temperature was elevated, the average particle size deviated from the crystal size as a result of the formation of relatively large agglomeration in the powders.

3.3. UV–vis diffuse absorption spectra of BiVO$_4$

Fig. 3 illustrates the UV–vis absorption spectra of the microemulsion- derived BiVO$_4$ heated at different temperatures and the solid-state derived BiVO$_4$ powders heated at 700 °C for 5 h. All the spectra of the prepared samples exhibited absorption in the visible and UV light regions. According to the intersection point of the tangent line and the x-axis shown in Fig. 3(a), the absorption edge of BiVO$_4$ heated at different temperatures was around

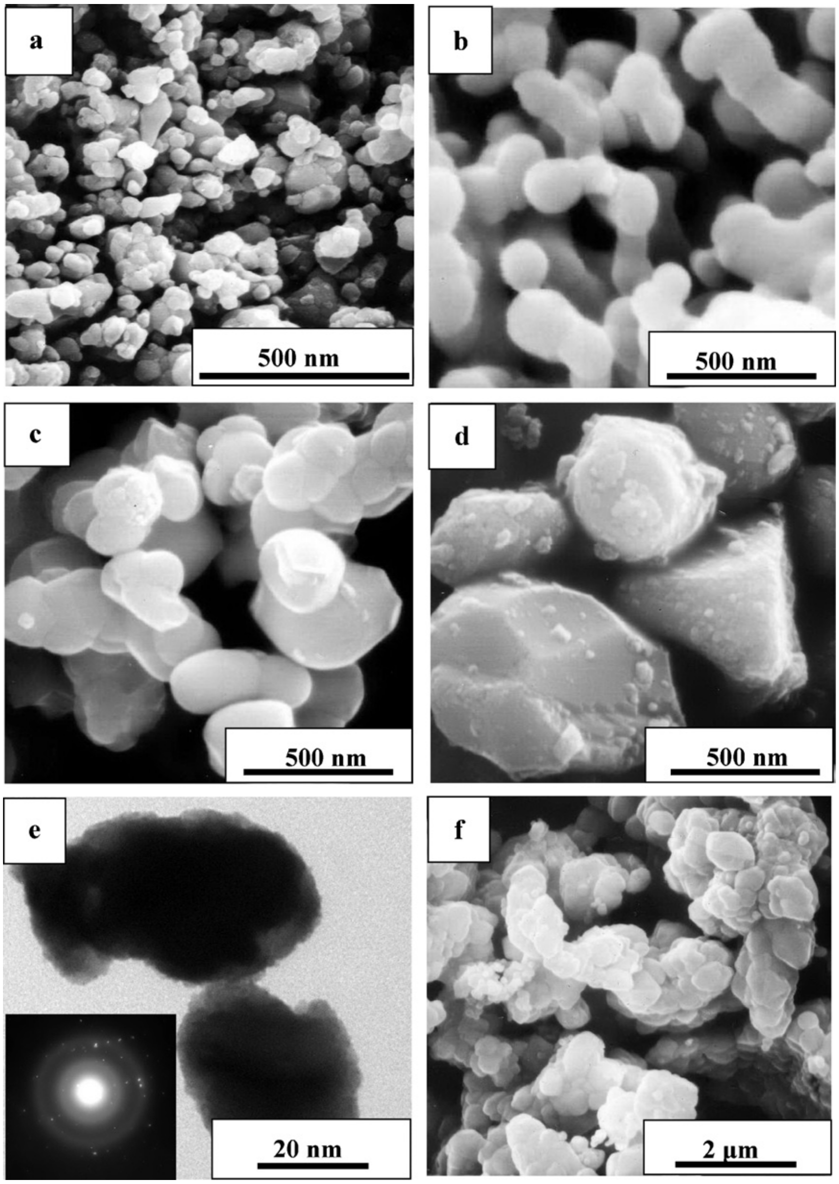

Fig. 2. Scanning electron micrographs of microemulsion-derived $BiVO_4$ powders heated at (a) 400, (b) 500, (c) 600 and (d) 700 °C for 20 min and solid-state derived $BiVO_4$ powders heated at (f) 700 °C for 5 h. (e) Transmission electron micrograph of microemulsion-derived $BiVO_4$ powders heated at 400 °C for 20 min.

544 nm. The corresponding band gap was estimated to be 2.28 eV, which is consistent with the band gap of monoclinic $BiVO_4$ of 2.4 eV [5–9]. The schematic diagram of band structure of $BiVO_4$ is shown in the inset of Fig. 3. For monoclinic sheelite $BiVO_4$, the absorption in UV light region is assigned to the electrons excited from O 2p valence band to V 3d (in $VO_4{}^{3-}$) conduction band. The visible-light absorption is due to the excitation of electrons from the valence band, owing to the hybridized Bi 6s and O 2p, to the V 3d conduction band. The largely dispersed valence band can facilitate the mobility of photoexcited holes, leading to enhanced photocatalytic activity [5,6,30,31].

3.4. Photocatalytic activity of $BiVO_4$

Fig. 4 illustrates the variation in the concentration of methylene blue solutions decomposed by the prepared photocatalysts under visible-light illumination. C_0 and C represent the initial and resultant concentrations of methylene blue solution, respectively. The values of normalized concentration C/C_0 after 4 h-irradiation of visible light were around 0.19, 0.68, 0.65 and 0.78 for the microemulsion-derived $BiVO_4$ powders heated at 400, 500, 600 and 700 °C, respectively. It is indicated that the microemulsion derived powders heated at 400 °C exhibited the highest activity. Only 2-h illumination was required to nearly decompose methylene blue completely. On the contrary, the value of C/C_0 after 4 h-irradiation of visible light was 0.83 for the solid-state derived $BiVO_4$ powders. The results demonstrate that the photocatalytic activity of the solid-state derived powders was significantly lower than that of the samples synthesized via the reverse-microemulsion process. Fig. 5 depicts the decolorization degree of $BiVO_4$ calcined at different heating temperatures in relation to the particle size. The decolorization degree was calculated via calibration between the measured absorbance and methylene blue solution concentration. The decolorization value can be obtained using the following equation:

$$D = \frac{1 - C}{C_0} \tag{2}$$

where D represents the decolorization degree, C_0 the initial methylene blue concentration, and C the final methylene blue con-

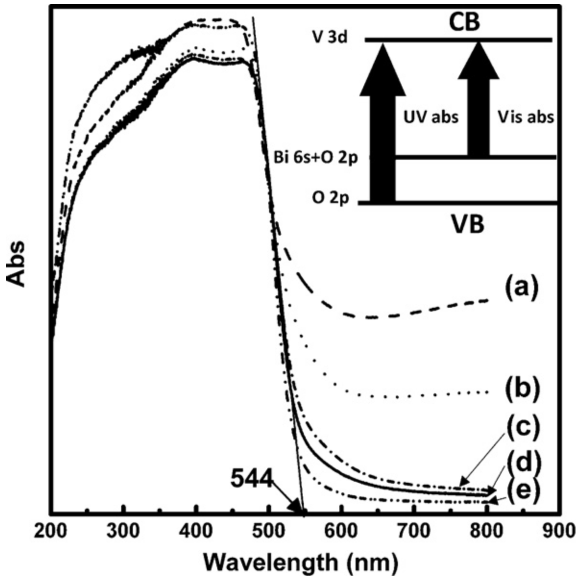

Fig. 3. UV–vis absorption spectra of microemulsion-derived $BiVO_4$ powders heated at (a) 400, (b) 500, (c) 600 and (d) 700 °C for 20 min and the solid-state derived $BiVO_4$ powders heated at (e) 700 °C for 5 h. Inset: the band structure of $BiVO_4$.

centration. It is seen that the photoactivity of the solid-state derived $BiVO_4$ was significantly lower than that of the microemulsion-derived $BiVO_4$. It is attributed to the fact that the powders of the solid-state derived $BiVO_4$ were aggregated seriously. Therefore, the surface area of the solid-state derived powders was lower than that of the microemulsion-derived powders. For the microemulsion-derived $BiVO_4$ powders, it is found that the photocatalytic activity decreased as the heating duration of the $BiVO_4$ powders increased. Elevating heating temperatures led to an increase in the crystallinity of $BiVO_4$ as shown in the inset of Fig. 5. The results indicate that particle size, as compared with crystallinity, is the dominant factor in influencing the photocatalytic activity. The nano-sized $BiVO_4$ powders derived from the microemulsion route exhibited superior photoactivity. Therefore, the reverse-microemulsion process was demonstrated to be a promising method for synthesizing visible-light-driven $BiVO_4$ with enhanced photocatalytic activities at low temperatures.

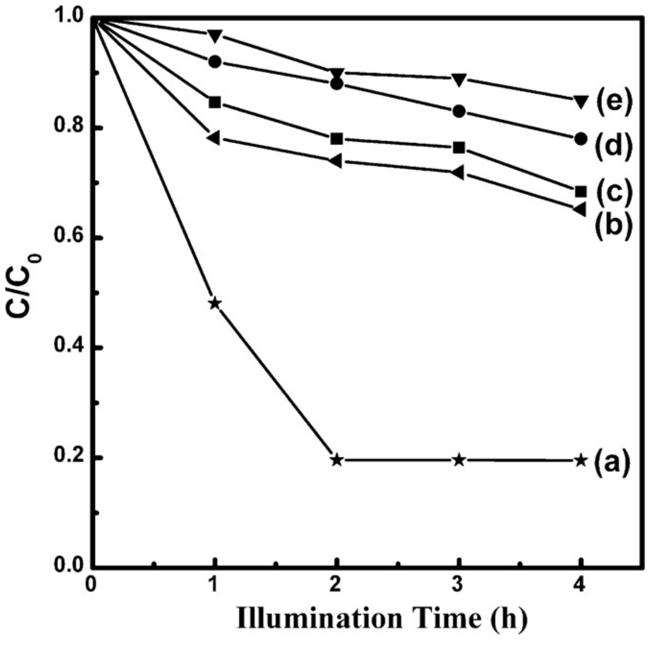

Fig. 4. Photocatalytic activities of microemulsion-derived $BiVO_4$ powders heated at (a) 400, (b) 600, (c) 500, (d) 700 °C and (e) the solid-state derived sample.

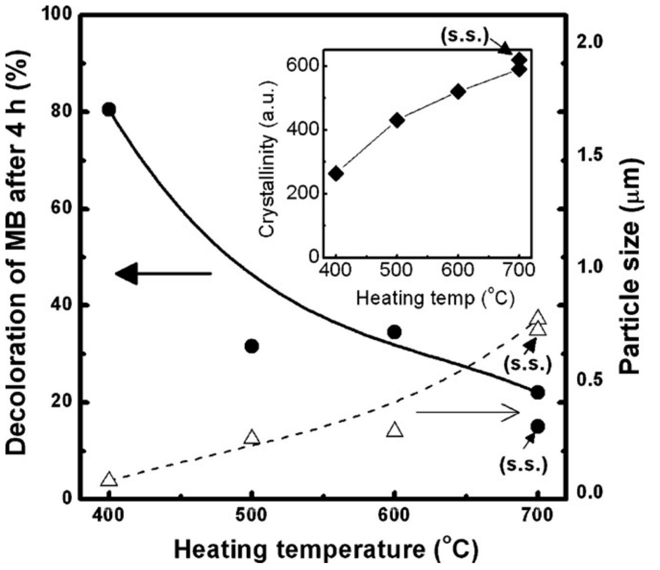

Fig. 5. Variation in decolorization of methylene blue, particle size and crystallinity of microemulsion-derived $BiVO_4$ heated at different temperatures and the solid-state derived $BiVO_4$ powders heated at 700 °C for 5 h after illumination for 4 h.

4. Conclusions

$BiVO_4$ nanoparticles with high crystallinity were successfully synthesized via the reverse-microemulsion process at a heating temperature as low as 400 °C. This process significantly reduced the heating time and temperature as compared with the solid-state and wet chemical techniques. The average particle size of the 400 °C-heated powders was around 35 nm. The powders prepared via the reverse-microemulsion process have smaller grain sizes and uniform microstructures as compared with those prepared via the conventional processes. The reduced particle size can be ascribed to the presence of nano-scaled micelles that restrict the growth of the particles. Under visible-light illumination, microemulsion-derived $BiVO_4$ powders exhibited superior photocatalytic activity than the solid-state derived powders. The reverse-microemulsion process was demonstrated to be a practical approach for preparing visible-light-driven $BiVO_4$ at relatively low temperatures.

References

[1] S.F. Chen, W. Zhao, W. Liu, S.J. Zhang, Appl. Surf. Sci. 255 (2008) 2478–2484.
[2] X.L. Wang, J.P. Tu, S.F. Wang, Y.F. Yuan, K.F. Li, J. Zhang, J. Alloys Compd. 462 (2008) 220–224.
[3] D.J. Yang, H.W. Liu, Z.F. Zheng, Y. Yuan, J.C. Zhao, E.R. Waclawik, X.B. Ke, H.Y. Zhu, J. Am. Chem. Soc. 131 (2009) 17885–17893.
[4] H. Chen, S. Chen, X. Quan, Y.B. Zhang, Environ. Sci. Technol. 44 (2010) 451–455.
[5] G.S. Li, D.Q. Zhang, J.C. Yu, Chem. Mater. 20 (2008) 3983–3992.
[6] D. Ke, T. Peng, L. Ma, P. Cai, P. Jiang, Appl. Catal. A 350 (2008) 111–117.
[7] L. Zhang, D.R. Chen, X.L. Jiao, J. Phys. Chem. B 110 (2006) 2668–2673.
[8] L. Zhou, W.Z. Wang, L. Zhang, H.L. Xu, W. Zhu, J. Phys. Chem. C 111 (2007) 13659–13664.
[9] B.P. Xie, H.X. Zhang, P.X. Cai, R.L. Qiu, Y. Xiong, Chemosphere 63 (2006) 956–963.
[10] L. Zhou, W.Z. Wang, H.L. Xu, Cryst. Growth Des. 8 (2008) 728–733.
[11] H.M. Luo, H.A. Mueller, M.T. McCleskey, K.A. Burrell, E. Bauer, Q.X. Jia, J. Phys. Chem. C 112 (2008) 6099–6102.
[12] Y. Zhao, Y. Xie, X. Zhu, S. Yan, S.X. Wang, Chem. Eur. J. 14 (2008) 1601–1606.
[13] H.Q. Jiang, H. Endo, H. Natori, M. Nagai, K. Kobayashi, J. Eur. Ceram. Soc. 28 (2008) 2955–2962.
[14] R. Strobel, H.J. Metz, S.E. Pratsinis, Chem. Mater. 20 (2008) 6346–6351.
[15] H. Xu, H. Li, C. Wu, J. Chu, Y. Yan, H. Shu, Z. Gu, J. Hazard. Mater. 153 (2008) 877–884.
[16] L. Ge, Mater. Chem. Phys. 107 (2008) 465–470.

[17] H. Xu, H. Li, C. Wu, J. Chu, Y. Yan, H. Shu, Mater. Sci. Eng. B 147 (2008) 52–56.
[18] L. Ge, Mater. Lett. 62 (2008) 926–928.
[19] H.Q. Jiang, M. Nagai, K. Kobayashi, J. Alloys Compd. 479 (2009) 821–827.
[20] L.Z. Li, B. Yan, J. Alloys Compd. 476 (2009) 624–628.
[21] C.H. Lu, H.C. Wang, J. Mater. Chem. 13 (2003) 428–431.
[22] X-ray Powder Data File, International Center of Diffraction Data, Card No. 83-1698 (1979).
[23] C.H. Lu, S.Y. Chen, C.H. Hsu, Mater. Sci. Eng. B 140 (2007) 218–221.
[24] C.H. Lu, H.C. Wang, J. Electrochem. Soc. 152 (2005), C 341–C 347.
[25] C.H. Lu, S.K. Saha, J. Am. Ceram. Soc. 83 (2000) 1320–1322.
[26] Y.K. Lin, C.H. Lu, J. Power Sources 189 (2009) 353–358.
[27] C.H. Lu, H.C. Wang, J. Eur. Ceram. Soc. 24 (2004) 717–723.
[28] A.J. Zarur, J.Y. Ying, Nature 403 (2000) 65–67.
[29] M.T. Weller, Inorganic Materials Chemistry, Oxford University Press, Oxford, UK, 1994.
[30] M. Oshikiri, M. Boero, J.H. Ye, Z.G. Zou, G. Kido, J. Chem. Phys. 117 (2002) 7313–7318.
[31] J.W. Tang, Z.G. Zou, J.H. Ye, Angew. Chem. Int. Ed. 43 (2004) 4463–4466.